

See discussions, stats, and author profiles for this publication at: <https://www.researchgate.net/publication/381301279>


# Pattern Synthesis and Digital Beamforming Capabilities of the Fully Digital Horus Radar

Conference Paper · May 2024  
DOI: 10.1109/RadarConf2458775.2024.10548659

CITATIONS  
6

READS  
310

4 authors, including:




David Schwartzman

University of Oklahoma

96 PUBLICATIONS 564 CITATIONS

SEE PROFILE




Robert D. Palmer

University of Oklahoma

317 PUBLICATIONS 4,382 CITATIONS

SEE PROFILE



Matthew Herndon

University of Oklahoma

13 PUBLICATIONS 130 CITATIONS

SEE PROFILE

# Pattern Synthesis and Digital Beamforming Capabilities of the Fully Digital Horus Radar

David Schwartzman<sup>1,2,3</sup> , Robert D. Palmer<sup>1,2,3</sup> , Matthew Herndon<sup>1</sup> , and Mark Yeary<sup>1,3</sup> 

<sup>1</sup>*Advanced Radar Research Center (ARRC), The University of Oklahoma*

<sup>2</sup>*School of Meteorology, The University of Oklahoma*

<sup>3</sup>*School of Electrical and Computer Engineering, The University of Oklahoma*

**Abstract**—The Horus radar program has received support from the University of Oklahoma, the NOAA National Severe Storms Laboratory, and the US DoD Office of Naval Research. The current work reports results from the Horus-NOAA radar, which is operational. The radar comprises a mobile, fully digital, polarimetric, S-band Phased Array Radar (PAR) developed from its inception to meet demanding mission-critical observational requirements for next-generation weather surveillance. In this paper, we present antenna pattern synthesis methods that exploit the beamforming capabilities of Horus. The measured Horus embedded element patterns are utilized in the synthesis to account for practical antenna performance. We investigate phase-only and constrained-loss magnitude/phase pattern synthesis methods to shape the transmit beam in various ways, including intentional beam broadening (“spoiling”) and beams with multiple simultaneous peaks in different directions. Results indicate that using synthesized beams with multiple simultaneous transmit peaks in different directions improves sidelobe isolation, producing two-way patterns similar to those from conventional single-beam operations. There is an inevitable loss in echo detectability (with respect to a full aperture pencil beam) due to the lower power density when spreading the mainlobe power. Evaluating these beamforming modes is critical for achieving high-temporal resolution polarimetric weather measurements with phased array radars.

**Index Terms**—pattern synthesis, digital phased array radar, polarimetric radar, radar imaging, element pattern

## I. INTRODUCTION

Phased Array Radar (PAR) technology is rapidly gaining recognition as a candidate technology for future weather radars capable of providing tailored, high-quality meteorological observations, crucial for advancing the understanding of atmospheric phenomena [1, 2]. Due to the limited visible region of a single-face planar PAR (typically  $\pm 45^\circ$  in antenna-boresight-relative  $\theta$  and  $\phi$  spherical coordinates), either multiple PAR faces (3 or 4) or mechanical scanning in azimuth are needed to provide full radar coverage. The single-faced rotating PAR architecture has emerged as a compromise solution to provide full coverage for weather surveillance. Although this solution offers a more affordable cost compared to a stationary four-faced PAR [3], it requires mechanical rotation in azimuth, which limits system capabilities.

The Horus radar was designed and built by the University of Oklahoma’s Advanced Radar Research Center (ARRC). It consists of a mobile, fully digital, polarimetric, S-band



Fig. 1. The Horus system, a mobile, fully digital, S-band polarimetric phased array weather radar.

PAR developed from its inception to achieve demanding mission-critical observational requirements for next-generation weather surveillance. The system has been operational since 2023. Its polarimetric capabilities involve the transmission and reception of electromagnetic waves in both Horizontal (H) and Vertical (V) polarizations, which are used to estimate weather radar variables. The concept of operations for the Horus radar involves using advanced beamforming concepts while mechanically rotating the antenna in azimuth. These advanced modes entail synthesizing custom antenna radiation patterns on transmission to simultaneously illuminate different regions and using digital beamforming (DBF) to form multiple receive beams from signals within the illuminated regions [4].

In this paper, we present progress towards a hybrid optimization method for synthesizing beam patterns using phase-only and constrained-loss magnitude/phase weights to exploit the beamforming capabilities of Horus. The measured Horus embedded element patterns are used in the synthesis to account for practical antenna performance. First, we investigate phase-only pattern synthesis to maximize antenna gain on transmission and shape the transmit beams in different ways. Smooth phase excitations across the array are expected to produce low sidelobe levels and are modeled here using a Bézier-surface parametrization. Next, we use a similar approach but allow the optimization to apply amplitude weights, constraining the

gain loss to a desired (e.g., 2 dB) value. Our interest lies in producing beamforming weights for intentional beam broadening (“spoiling”) and for beams with multiple simultaneous or quasi-simultaneous peaks in different directions [5, 6]. Simulations show that Horus can synthesize one- and two-dimensional spoiled beams, and beams with multiple simultaneous peaks in different directions effectively. Key results indicate that using synthesized beams with multiple simultaneous transmit peaks in different directions helps improve sidelobe isolation, producing two-way patterns similar to those from a conventional single-beam operation. Evaluating these advanced beamforming modes is critical for high-temporal resolution polarimetric weather measurements with PARs.

## II. THE FULLY DIGITAL HORUS RADAR

Horus is based on the most advanced digital PAR architecture, a fully digital design [2]. In this system, every element and polarization has its own transmitter and receiver to provide maximum flexibility in terms of beamforming and software reconfigurability. This radar is considered an *engineering* demonstrator with the goal of mitigating risks associated with fully digital phased array architectures and demonstrating advanced capabilities. Its size and operating frequency (see Table I) limit the beamwidth to  $\sim 3.5^\circ$  (i.e., with taper), which is not adequate to resolve complex structures in most severe weather precipitation systems that are far from the radar. However, its inherent scalable design allows the demonstration of overall functionality while considering plans for future full-scale systems. More details about Horus can be found in [7].

TABLE I  
SPECIFICATIONS OF THE HORUS RADAR

|                                |                                      |
|--------------------------------|--------------------------------------|
| Frequency                      | 2.7–3.1 GHz                          |
| Polarization                   | ATSR/STSR/RHCP/LHCP                  |
| Tx Waveform                    | Arbitrary Waveform Generator         |
| Tx Peak Power (single element) | 10 W/polarization                    |
| Max Tx Pulse Width             | 100 $\mu$ s @ 10% duty cycle         |
| Max Tx Bandwidth               | 100 MHz                              |
| Element Spacing                | 0.5 $\lambda$ @ 2.951 GHz            |
| Number of Panels               | 25 (1600 elements)                   |
| Max Electronic Scan Angle      | $\pm 45^\circ$ az, $\pm 45^\circ$ el |
| Aperture Size                  | $2.03 \times 2.03$ m <sup>2</sup>    |
| Tx/Rx Beamwidth Broadside      | $2.58^\circ$ (no taper)              |
| Detectability (1 pulse)        | 4.3 dBZ @ 50 km                      |

The proposed hybrid beam synthesis optimization requires an estimate of the embedded element pattern. It is used to 1) accurately account for scan loss and compensate for gain differences on transmit beams, and 2) to account for differences in the H/V patterns and produce polarization-dependent phase weights so that farfield synthesized patterns are matched [8]. The following section describes our element pattern measurements used to estimate the embedded element pattern.

### A. Element Pattern Measurements

The Horus antenna element patterns were characterized in the ARRC’s precision anechoic chamber using the spherical

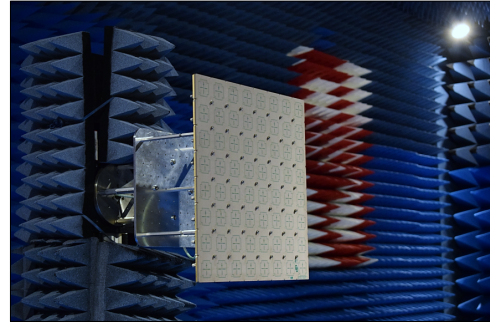


Fig. 2. Front view of the Horus antenna panel mounted in the anechoic chamber positioner.

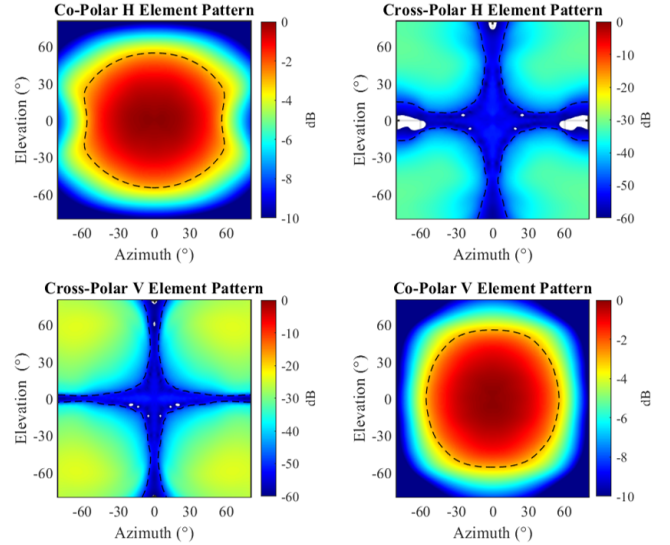


Fig. 3. Measured Horus embedded element patterns. Dotted black contour lines represent the -3 dB and -50 dB levels in the co- and cross-polar patterns.

far-field scan mode. One  $8 \times 8$  dual-polarization antenna panel was mounted on a positioner that rotates in the spherical coordinate system, for full (two-dimensional) characterization of the element patterns. The setup is illustrated in Fig. 2.

The S-band probe used by the chamber scanner received signals transmitted from the Horus panel itself, thereby ensuring coherence with this fully digital array. With this setup, the performance of each antenna element was individually measured with  $5^\circ \times 5^\circ$  sampling in the spherical system for a total of  $64 \times 2 = 128$  measurements. While each individual element was being measured, all others were terminated with matched impedances to emulate the behavior of a fully connected panel (although only one element was excited at a time). This setup can only characterize the passive behavior of the antenna, as it does not include the effects of the radar front-end transceivers. These effects have been characterized recently, showing excellent agreement with passive antenna measurements, and reported along with a new polarimetric calibration method based on the holographic back-projection of electric fields [9].

Magnitude and phase measurements were obtained for each element at 21 frequencies (2.95 – 3.15 GHz, in steps

of 0.01 GHz; centered at 3.05 GHz), and for the copolar and cross-polar antenna radiation patterns. Through digital post-processing, data from corresponding polarizations were properly beamformed and compared to ANSYS HFSS panel simulations to verify the patterns of the Horus panel. The measured cross-polarization levels (with respect to the copolar peak) at the intended transmit frequency (3.05 GHz) are -50.14 dB on broadside.

### B. Derived Embedded Element Pattern

Embedded element patterns are critical to characterize the phased array antenna performance. Using the individual Horus element patterns measured, we derived the embedded element patterns of the antenna shown in Fig. 3. Note that these are presented in the Ludwig-II coordinate system (azimuth/elevation). These measurements serve as a basis for full array patterns to be calculated. A qualitative comparison of the copolar patterns (main diagonal in Fig. 3), indicates good matching between the H and V patterns.

Embedded element patterns also provide key information about cross-polarization levels that can be achieved with the array, ultimately determining polarimetric-estimation performance. This is especially the case at steering angles away from the array's principal planes, given that cross-polarization levels increase with the angle moving away from these planes. The element patterns show cross-polar levels lower than -50 dB along the principal planes. Normally, these levels are lowered when thousands of elements are arranged in the array, as random phase errors create incoherent interference, producing deeper nulls. Away from the principal planes, cross-polarization levels increase up to approximately -20 to -25 dB. A new technique recently developed for the Horus system, the "Cross-polar Canceller (XPC)" [10], can mitigate cross-polar contamination away from the principal planes. It leverages a subset of designated canceller elements to transmit a waveform with 180° phase shift from that in the cross-polar fields to electromagnetically mitigate it.

Having individual H and V embedded element patterns allows the prediction of different steered and tapered antenna array patterns, but more importantly, allows modeling the performance of the full Horus array. Using these measurements and the Horus antenna architecture, full Horus array patterns are simulated using the procedure in the next section.

## III. BEAM PATTERN SYNTHESIS

Active PARs can synthesize custom beam patterns on transmission and reception by modulating the magnitude and phase of signals from each antenna element. This capability can be used to produce different transmit beams for advanced scanning modes, at the expense of increased sidelobe levels, reduced gain, and slightly increased beamwidth (compared to a pencil beam). It is preferable to use phase-only weights to synthesize the transmit beams and minimize gain loss, especially for estimating parameters from relatively weak meteorological returns. Various methods have been developed for the solution of the phase-only synthesis problem [8].

Although it is preferable to use phase-only weights, this may limit the degrees of freedom for beam shaping and the attainable sidelobe levels. A constrained-loss magnitude and phase synthesis method is also applied here, for synthesizing beam patterns with simultaneous peaks spaced in angle.

We begin by modeling the array factor of a planar PAR as follows,

$$AF(\theta, \phi) = \sum_{m=1}^M \sum_{n=1}^N w_{mn} e^{j\phi_{mn}} e^{-jm\Psi_x} e^{-jn\Psi_y} \quad (1)$$

where  $0 \leq w_{mn} \leq 1 \in \mathbb{R}$  and  $\phi_{mn} \in (-\pi, \pi]$  are the magnitude and phase weights for the element in row  $m$  column  $n$ ,  $\Psi_x = kd_x \sin(\theta) \cos(\phi)$ ,  $\Psi_y = kd_y \sin(\theta) \sin(\phi)$ ,  $k = 2\pi/\lambda$  is the wavenumber,  $\lambda$  is the wavelength,  $d_x$  and  $d_y$  are the element spacings in  $x$  and  $y$ , and  $\theta/\phi$  are the steering angles. Herein, we assume that  $d_x = d_y = \lambda/2$ . We are interested in searching for optimal values for  $w_{mn}$  and  $\phi_{mn}$ , to synthesize different transmit patterns.

The array pattern can be approximated using the embedded element power patterns as [11],

$$F^{pq}(\theta, \phi) = F_e^{pq}(\theta, \phi) |AF(\theta, \phi)|^2 \quad (2)$$

where  $F_e^{pq}(\theta, \phi)$  represents the embedded element pattern, and  $p$  and  $q$  could be either  $H$  or  $V$  representing the horizontal or vertical polarizations. With the previous expression, we can obtain the four patterns in the polarization scattering matrix, namely,  $F^{HH}$  (copolar H),  $F^{HV}$  (cross-polar H),  $F^{VV}$  (copolar V), and  $F^{VH}$  (cross-polar V), as in Fig. 3. It should be noted that the use of the embedded element pattern to represent the full array is only an approximation, because it neglects diffraction (edge) effects.

We use a global optimization solver to search for phase weights that produce a synthesized beam with maximum efficiency and meeting a prescribed antenna pattern envelope function. An efficiency metric is introduced as the ratio of the synthesized pattern gain over the pencil-beam gain (i.e., uniform weights) to quantify the synthesis gain loss. An antenna pattern envelope function is designed to control 1) the 3-dB width of the transmit beam, and 2) the sidelobe levels as a function of azimuth and elevation in the visible region. The efficiency loss (EL) is the integrated power difference between the synthesized pattern half-power beamwidth ( $\theta_1$ , defined by  $F^{pp} > 0.5 = -3$  dB) and a normalized gain value of 1 (0 dB), expressed in dB as,

$$EL = -10 \log_{10} \left[ \iint_{F^{pp} > 0.5} \min[F^{pp}, E] \sin(\theta) d\theta d\phi \right] \text{ (dB)},$$

and the integrated contamination (IC) is the volume of the synthesized pattern that exceeds a predefined pattern design envelope,  $E(\theta, \phi)$ , defined in dB as,

$$IC = 10 \log_{10} \left[ \frac{1}{2\pi^2} \int_{-\pi/2}^{\pi/2} \int_{-\pi}^{\pi} \frac{\max[F^{pp}, E]}{E} \sin(\theta) d\theta d\phi \right] \text{ (dB)}.$$

Note that we dropped the angular dependence of  $F^{pq}$  and  $E$  (i.e.,  $\theta$  and  $\phi$ ) to simplify notation. If the synthesized antenna pattern is below the predefined envelope, the IC is 0 dB. Similarly, if the mainlobe of the antenna pattern is identically 1 in linear units (i.e., 0 dB), the EL is 0 dB. The optimization is then posed as follows,

$$\min_{\substack{\phi_{m,n} \in [-\pi/2, \pi/2] \\ 0 \leq w_{m,n} \leq 1}} 12 \text{ IC} + \text{EL} \quad (3a)$$

$$\text{subject to} \quad 10 \log_{10} \left[ \frac{\sum_{m,n} |w_{m,n}|^2}{N} \right] \geq L, \quad (3b)$$

where  $L$  is the maximum gain loss desired (from amplitude tapering) in dB (e.g., -2 dB),  $N$  is the total number of elements in the array.

Given the relatively large number of beamforming coefficients to be optimized (i.e., two real numbers per antenna element per polarization), weights are parameterized using Bézier surfaces. These surfaces are defined by a small number of “control points” that use Bernstein polynomials as basis functions to produce smooth surfaces over a desired domain. In the proposed optimization, one control point is placed every 2 elements in each array dimension.

#### IV. OPTIMIZED ARRAY PATTERNS

In this section we illustrate the performance of the proposed optimization to synthesize different transmit beams. The genetic algorithm solver in MATLAB was used. The goal is to reduce the volume scan time with minimum impact to polarimetric weather data quality.

##### A. Broad Transmit Beams

First, we derive two-dimensional envelope functions to design a beams intentionally broadened (or “spoiled”) in elevation. Three beams are optimized for beamwidths of  $10^\circ$ ,  $15^\circ$ , and  $20^\circ$  in elevation. The envelope function sets the peak one-way sidelobe levels to -15 dB. In this case, we produce *phase-only* beamforming coefficients, hence,  $w_{m,n} = 1 \ \forall \ m, n$  and

$L = 0$  dB. That is, since no amplitude taper is used, there is no additional loss incurred beyond that of the synthesis efficiency (minimized with the EL).

The genetic-algorithm solver converged to feasible solutions for all three beams specified. The outputs are sets of two-dimensional phase weights, which produce the synthesized beam pattern cuts (spoiled only in elevation) shown in Fig. 4.

A close look at the patterns shows wide transmit beams, all with peak sidelobe levels below -15 dB in elevation, and a relatively small ripple across the mainlobe peak ( $< 0.3$  dB). The IC of all three patterns shown here is 0 dB, meaning they are within design expectations. These are example beams synthesized with the described method, and other beam shapes (e.g., a cosecant beam) could be designed for air surveillance applications. Broadening the transmit beam can reduce antenna gain considerably, resulting in the loss of sensitivity in detecting relatively weak weather returns.

##### B. Multiple Simultaneous Beams

The scan time reduction could also be achieved by synthesizing a transmit beam with multiple simultaneous peaks in different directions and forming receive beams in those directions. The pattern synthesis optimization can produce weights for multiple beams with different angular spacing, going from a few degrees up to at least  $\pm 30^\circ$  and possibly more. We illustrate the output of our optimization framework by synthesizing a beam with three simultaneous beams in elevation spaced by  $15^\circ$  (i.e., at  $-15^\circ$ ,  $0^\circ$ , and  $15^\circ$  with respect to broadside). In this case, the we use the constrained-loss method, allowing a maximum loss of 2 dB ( $L = -2$  dB in eq. 3b). The synthesized beam pattern cuts are shown in Fig. 5.

Digital beamforming is used to form three simultaneous beams on receive at different steering angles. Traditional beamforming methods (e.g., Fourier beamforming) are generally effective at producing low-sidelobe two-way beam patterns. Transmit beams with wider angle spacing (azimuth or

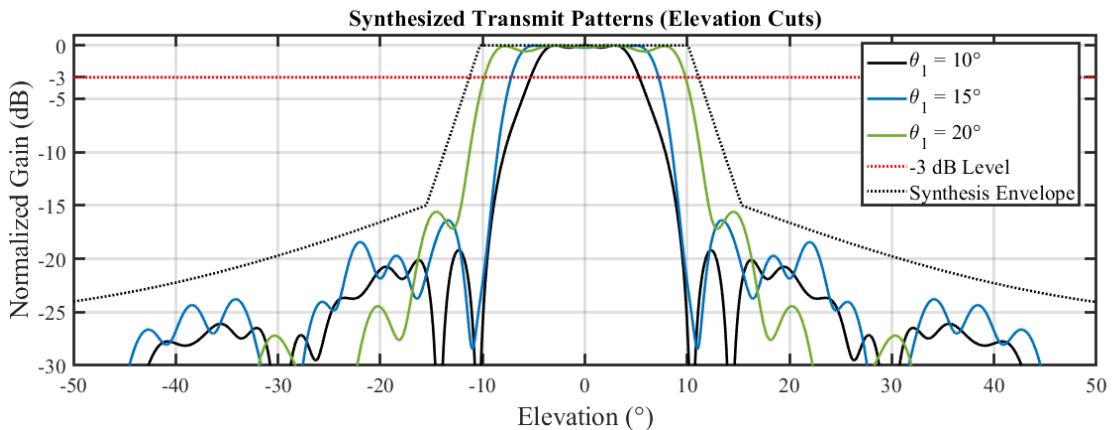


Fig. 4. Synthesized spoiled transmit antenna patterns obtained by applying the optimized phase-only weights to the current Horus array architecture (13 panels).



elevation) reduce the coupling among multiple transmit/receive beams, due to the fall-off with the angle of the one-way antenna pattern sidelobe structure. One way to further reduce the undesired returns is to apply pre-computed weights to the digital receive channels that minimize the array response at the angles of the interfering transmit beams. The effectiveness of this method is illustrated in Fig. 6, where deterministic nulls are placed in directions coinciding with 2 out of 3 transmit beam peaks at a time. If the array is perfectly calibrated the nulls placed on the receive pattern can be extremely deep, and would lower the two-way response below -60 dB at the angles of the interfering transmit beams. Randomly failed TR elements and calibration errors can significantly reduce the effectiveness of the nulling unless the locations of the failed elements are known and used in determining the appropriate weights. Assuming measured Horus calibration errors ( $\sigma_a = 0.5$  dB and  $\sigma_p = 2^\circ$ ), the improvement is still considerable and results in two-way sidelobe levels below -45 dB with respect to the normalized mainlobe peak.

### C. Multiple Time-Concatenated Beams

Another option to reduce the scan time is to transmit time-concatenated simultaneous H/V pencil beams in different directions while simultaneously forming receive beams [6]. Using this method, full-directivity sub-pulses are successively transmitted in the directions of each receive beam (although the duty cycle could be a limiting factor). Horus supports sub-pulses with arbitrary widths and steering angles, allowing adaptive scanning concepts. After all sub-pulses have been transmitted, the digitally formed receive beams are formed simultaneously by listening to returns from each of the transmit directions, similar to the previous case (Fig. 6). A pulse transmission timing diagram for this mode is shown in Fig. 7, where each pulse is associated with a different transmit beam.

This mode is similar to the multiple simultaneous beams mode, in the sense that it transmits several beams spaced out in angle. As in the previous case, this helps improve sidelobe isolation, producing two-way patterns similar to those from a conventional single-beam operation. One important benefit over the mode with multiple simultaneous beams is

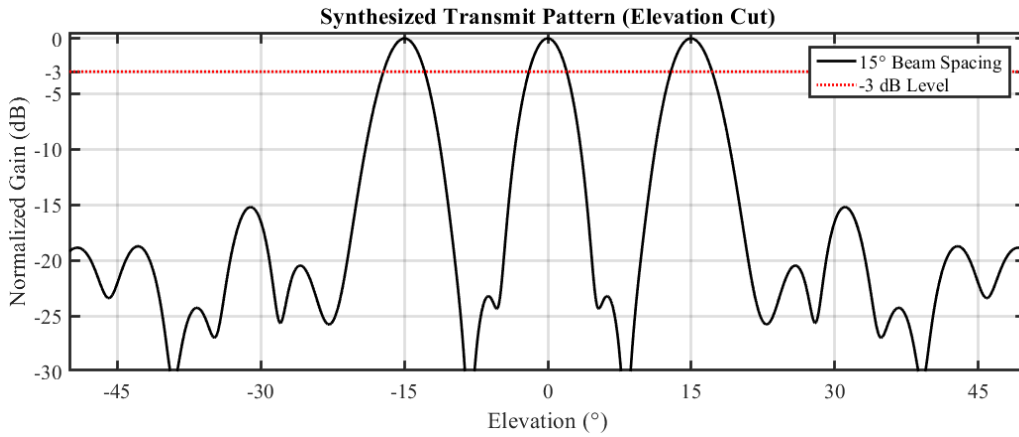


Fig. 5. Synthesized transmit antenna pattern with 3 simultaneous peaks in different directions, with beams spaced by  $15^\circ$  (i.e., at  $-15^\circ$ ,  $0^\circ$ , and  $15^\circ$  with respect to broadside).

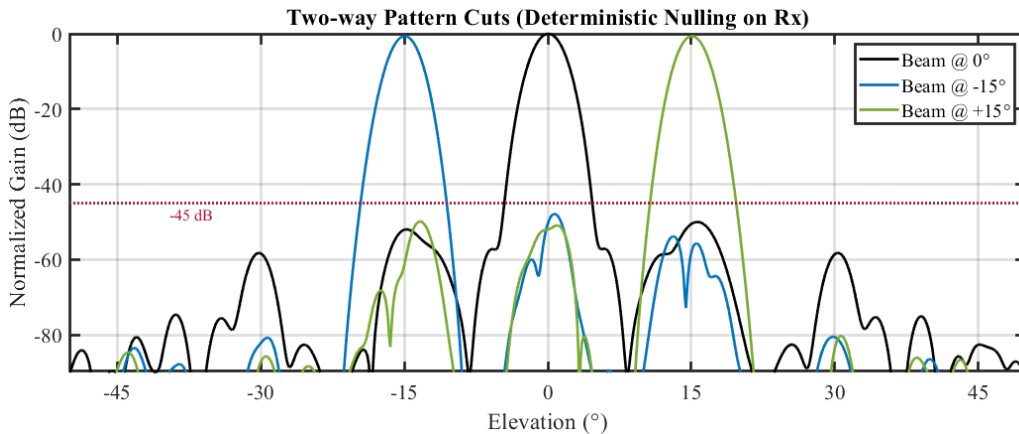


Fig. 6. Cuts along the elevation plane of the two-way beam patterns, where optimized nulls were placed on receive beams to reduce contamination from the transmit peaks in Fig. 5. Note that this simulation includes amplitude and phase errors (with  $\sigma_a = 0.5$  dB and  $\sigma_p = 2^\circ$ ), and a 2% random element failures.

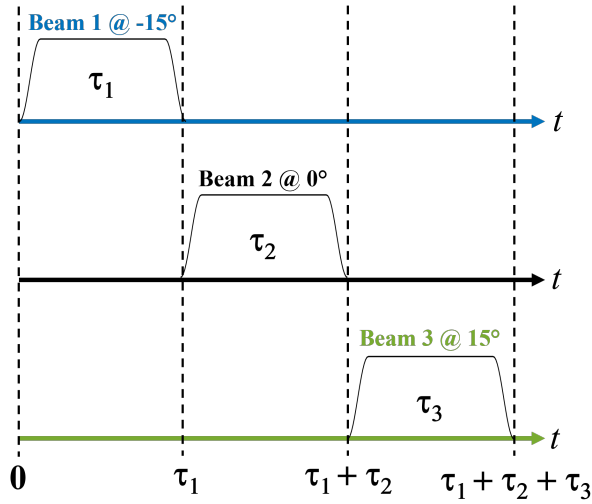


Fig. 7. Pulse transmission timing diagram for the mode with multiple concatenated transmit beams, showing the 3 time-concatenated pulses of arbitrary widths (i.e.,  $\tau_1 - \tau_3$ ). Each pulse is associated with a different transmit beam.

that in this case full transmit antenna gain is used for each of the concatenated beams. Furthermore, synthesizing these beams on transmission is trivial since they are nothing but conventional pencil beams steered in angle and transmitted back to back.

## V. CONCLUSION

This paper presents a hybrid optimization method for synthesizing beam patterns using phase-only and constrained-loss magnitude/phase weights to exploit beamforming capabilities of Horus. The measured Horus embedded element patterns are used in the synthesis to account for practical antenna performance. The pattern synthesis optimization is driven by a two-dimensional angular envelope function that shapes the mainlobe and limits the sidelobe levels. It also includes an efficiency factor to maximize synthesis performance and reduce ripple across the mainlobe. We use a genetic algorithm solver to search for a globally optimum weight vector (with magnitude and phase coefficients). The number of variables in the optimization is reduced by parametrizing the weights through Bézier surfaces that create smooth variations in the excitation applied across elements in the array. Preliminary results show that the proposed algorithm can be used to synthesize different types of transmit beam patterns.

We investigate the design of patterns with intentional beam broadening and beams with multiple simultaneous or quasi-simultaneous peaks in different directions. Our preliminary results show that Horus can synthesize two-dimensional spoiled beams, and beams with multiple simultaneous peaks in different directions effectively. Key results indicate that using synthesized beams with multiple simultaneous transmit peaks in different directions show higher two-way performance compared to spoiled beams. That is because transmit beams with wider angle spacing (azimuth or elevation) reduce the coupling among multiple transmit/receive beams, due to the fall-off with

the angle of the one-way antenna pattern sidelobe structure. It effectively improves sidelobe isolation and produces two-way patterns similar to those from a conventional single-beam operation (i.e., better angular resolution). The algorithm can produce transmit beams with one-way peak sidelobe levels at least 15 dB below the pattern peak and that meet a pattern-design envelope functions. There is, however, an inevitable loss in echo detectability when using these transmit beams (with respect to a full aperture pencil beam) due to the lower power density when spreading the mainlobe power. Evaluating these advanced beamforming modes is critical for high-temporal resolution polarimetric weather measurements with phased array radars.

## VI. ACKNOWLEDGEMENT

This work is supported primarily by NOAA/Office of Oceanic and Atmospheric Research under NOAA-University of Oklahoma Cooperative Agreement #NA21OAR4320204, U.S. Department of Commerce. It is also partially supported from the U. S. Office of Naval Research under award numbers N00014-19-1-2326 and N00014-20-1-2851. Special thanks to the ARRC's engineering staff for their dedication to the project.

## REFERENCES

- [1] D. S. Zrnic *et al.*, "Agile-Beam Phased Array Radar for Weather Observations," *Bull. of the American Meteorological Society*, vol. 88, no. 11, pp. 1753–1766, Nov. 2007. DOI: 10.1175/BAMS-88-11-1753.
- [2] R. Palmer *et al.*, "A Primer on Phased Array Radar Technology for the Atmospheric Sciences," *Bulletin of the American Meteorological Society*, vol. 103, no. 10, E2391–E2416, 2022. DOI: <https://doi.org/10.1175/BAMS-D-21-0172.1>.
- [3] D. Schwartzman, "Signal Processing Techniques and Concept of Operations for Polarimetric Rotating Phased Array Radar," Available at <https://hdl.handle.net/11244/326580>, Ph.D. dissertation, The University of Oklahoma, Norman, OK, USA, 2020.
- [4] D. Schwartzman *et al.*, "Distributed Beams: Concept of Operations for Polarimetric Rotating Phased Array Radar," *IEEE Trans. on Geoscience and Remote Sensing*, pp. 1–19, E2391–E2416, 2021. DOI: 10.1109/TGRS.2020.3047090.
- [5] V. M. Melnikov, R. J. Doviak, and D. S. Zrnić, "A method to increase the scanning rate of phased-array weather radar," *IEEE Transactions on Geoscience and Remote Sensing*, vol. 53, no. 10, pp. 5634–5643, Oct. 2015. DOI: 10.1109/TGRS.2015.2426704.
- [6] D. Schwartzman, M. Weber, S. Torres, H. Thomas, D. S. Zrnic, and I. Ivic, "Scanning concepts and architectures supporting rotating meteorological phased-array radar," in *101st American Meteorological Society Annual Meeting*, AMS, 2021.
- [7] R. D. Palmer *et al.*, "Horus—A Fully Digital Polarimetric Phased Array Radar for Next-Generation Weather Observations," *IEEE Transactions on Radar Systems*, vol. 1, pp. 96–117, 2023. DOI: 10.1109/TRS.2023.3280033.
- [8] D. Schwartzman *et al.*, "A Hybrid Antenna Pattern Synthesis Method for the Polarimetric Atmospheric Imaging Radar (PAIR)," in *2022 IEEE Radar Conference (RadarConf22)*, 2022, pp. 01–06. DOI: 10.1109/RadarConf2248738.2022.9764359.
- [9] D. Schwartzman, J. D. D. Díaz, D. Zrnić, M. Herndon, M. B. Yeary, and R. D. Palmer, "Holographic back-projection method for calibration of fully digital polarimetric phased array radar," *IEEE Transactions on Radar Systems*, vol. 1, pp. 295–307, 2023. DOI: 10.1109/TRS.2023.3286849.
- [10] C. Salazar, D. Schwartzman, B. Cheong, and R. D. Palmer, "A Novel Cross-Polar Cancellation for Improved Polarimetric Performance of Fully Digital Phased Array Radar," *IEEE Transactions on Radar Systems*, vol. Under Review, 2023.
- [11] R. J. Mailloux, *Phased Array Antenna Handbook*. Artech house, 2017.